METALLURGY AND FOUNDRY ENGINEERING – Vol. 31, 2005, No. 1

Edward Fraś*, Marcin Górny**, Hugo F. López***

SOLIDIFICATION CONDITIONS OF GRAY AND WHITE CAST IRON. PART II – EXPERIMENTAL VERIFICATION

1. INTRODUCTION

The structural quality of cast iron produced in the foundry industry is among other things assessed through evaluations of its chill and chilling tendency CT. Diverse methods are commonly employed in the foundry industry for testing the chill of cast iron. Among these methods, the A 367-55T ASTM chill-plate and chill-wedge testing techniques are the most widely known. Nevertheless, the chill of cast iron can also be assessed using pins [1], or plates with various size sections. These methods are employed in testing castings of various sizes in order to simulate influence of different cooling rates. Since the number of potential applications for cast iron is strongly dependent on its inherent CT, considerable efforts have been made in correlating its chill and CT values with metallurgical processing factors [2–4] or thermal analysis [5].

In part I of this work an expression was derived which can be used for predictions of the critical casting module below, which a chill develops. This condition is given by

$$M_{cr} = \frac{V_{cr}}{F_{cr}} \tag{1}$$

The above expression can also be described by

$$M_{cr} = p\mathrm{CT} \tag{2}$$

* M.Sc., **Ph.D., Faculty of Foundry Engineering, AGH University of Science and Technology, Reymonta 23, 30-059 Kraków, Poland; edfras@agh.edu.pl; ** Author is an award holder of the NATO Science Fellowship Programme, mgorny@agh.edu.pl

*** Prof., Department of Materials Engineering, University of Wisconsin-Milwaukee, P.O. Box 784, Milwaukee, WI 53201, USA; hlopez@uwm.edu

In addition, the wedge value for wedge shaped castings can be given by

$$w = \frac{4np}{\cos(\beta/2)}\,\mathrm{CT} \tag{3}$$

where:

$$p = \frac{2^{5/6}\, a\; T_s^{1/2}}{\pi\, \phi^{1/2} c_{ef}^{1/3}\; L_e^{1/6}} \tag{4}$$

V_c and F_c – the volume and surface area of the casting, respectively,
a – the mould ability to absorb heat,
n – the wedge coefficient,
T_s – the equilibrium temperature for the graphite eutectic (Eq. (11)),
c_{ef} – the effective specific heat of pre-eutectic austenite (Eq. (21) [12]),
ϕ – the heat coefficient of the metal (Eq. (28) [12]),
L_e – the latent heat for graphite eutectic,
β – the wedge angle (Fig. 7 [12]).

Two cases are clearly distinguished depending on the available information:

1) the nucleation coefficient b [^{o}C] (Eq. (13) [12]) and the density of sites (substrates) N_s [1/cm^3] for graphite nucleation are known; under these conditions CT can be described by

$$\mathrm{CT} = \left[\frac{1}{N_s\; \left(1 - f_\gamma\right) \mu_g^3\; \Delta T_{sc}^8} \exp\left(\frac{b}{\Delta T_{sc}} \right) \right]^{1/6} \tag{5}$$

2) the number of graphite eutectic cells N_g is directly available at $T \approx T_c$, then

$$\mathrm{CT} = \left[\frac{1}{N_g\; \left(1 - \mathrm{f}_\gamma\right) \mu_g^3\; \Delta T_{sc}^8} \right]^{1/6} \tag{6}$$

where:

ΔT_{sc} – the temperature range under which only graphite eutectic solidifies ($\Delta T_{sc} = T_s - T_c$) (see Fig. 2 and Eq. (69) [12]),
T_c – the temperature for cementite eutectic formation (Eq. (12)),
f_γ – the volume fraction of pre-eutectic austenite (Eq. (70) [12]),
μ_g – the growth coefficient for graphite eutectic (Eq. (68) [12]).

In cast iron, the chill and chilling tendency are closely related to the solidification conditions. It is well known, that the CT depends among other factors on the number of nucleation sites available for the formation of graphite eutectic cells during the solidification

process. A typical measurement of the number of active sites can be directly obtained from the density of eutectic cells (i e., each graphite nucleus gives rise to a single eutectic cell) or the nucleation coefficients (b and N_s), which account for the graphite nucleation potentials for a given casting [6, 7].

In this work, a series of experiments are carried out which are intended to corroborate the proposed theory on the eutectic cell count, chill and CT of cast iron. The experimental work is mainly based on thermal analysis and on measurements of chill and eutectic cell count, as well as the on determination of the nucleation coefficients.

2. EXPERIMENTAL PROCEDURE, RESULTS AND DISCUSSION

Small wedges and plates – Series I

In this part of the work, experimental melts were made in an electric induction furnace of intermediate frequency in a 15 kg capacity crucible. The raw materials were pig iron, steel scrap, commercially pure silicon, sulfur and ferro-phosphorus in amounts of 12 kg, 3 kg, 0.190 kg, 0.01 kg, and 0.03 kg, respectively. Melting was followed by liquid iron superheating up to 1420°C and inoculation using FOUNDRYSIL (73–75% Si, 0.75% Al, 0.75–1.25% Ca, 0.75–1.25% Ba) with a 0.2–0.5 cm granulation, and added as 0.5 % of the total charge weight. After various time intervals (1.5; 5; 10; 15; 20 and 25 minutes) from the end of inoculation treatment, the cast iron was poured into plate shaped moulds of s = 0.6; s = 1.0; s = 1.6; s = 2.2 and s = 3.0 cm in thickness. For the plates with 0.6; 1.0 and 1.6 cm in thickness, the length and height were 10 cm, while it was 14 cm for all the remaining plates. In all of the cases, the plates had a common gating system.

The foundry moulds were prepared using conventional moulding sand. In addition, they were instrumented with Pt/PtRh10 thermocouples enclosed in quartz sleeves of 0.16 cm in diameter for plates of 0.6 and 1 cm in thickness, and of 0.3 cm in diameter for plates of other thicknesses. The thermocouple tips were located in the geometrical center of each mold cavity perpendicularly to the heat transfer flow to improve the measurement accuracy. An Agilent 34970A electronic module was employed for numerical temperature recording. Figure 1 shows some typical cooling curves. These curves were then used for determinations of the initial metal temperature (T_i) just after filling of mould, and then the ϕ coefficient (see Eqs. (20), (21), (28) and (29) in [12]) could be calculated.

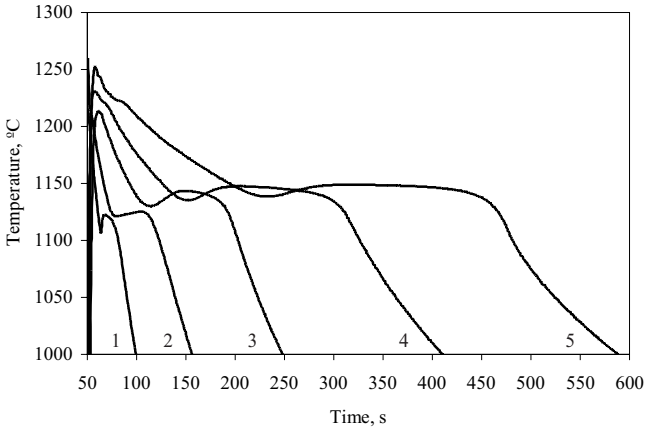

Fig. 1. *Cooling curves for cast iron and initial temperature of the metal in the mold cavity just after pouring T_i. Curves 1–5 – plates: s = 0.6, s = 1.0, s = 1.6, s = 2.2 and s = 3 cm*

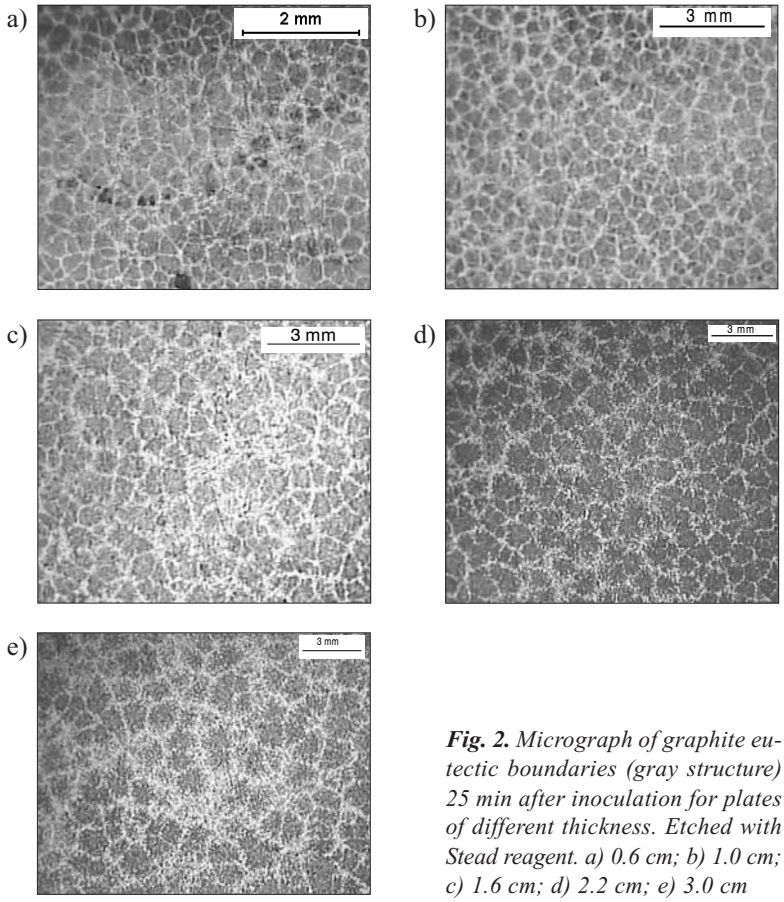

Fig. 2. *Micrograph of graphite eutectic boundaries (gray structure) 25 min after inoculation for plates of different thickness. Etched with Stead reagent. a) 0.6 cm; b) 1.0 cm; c) 1.6 cm; d) 2.2 cm; e) 3.0 cm*

After cooling, specimens for metallographic examination were taken from the geometrical centers of the plates. Metallographic examinations were made on polished and etched (Stead reagent) specimens to reveal graphite eutectic cell boundaries. Figure 2 shows a typical planar microstructure (on the specimen cross-section), with distinct eutectic cells. The planar microstructure is characterized by the cell count N_F (cell density), which gives the average number of graphite eutectic cells per unit area. The N_F parameter can be determined by means of the, so-called variant II of the Jeffries method, and applying the Saltykov formula as an unbiased estimator for the rectangle S of observation [8]

$$N_F = \frac{N_i + 0,5\, N_w + 1}{F} \tag{7}$$

where:

N_i – the number of eutectic cells inside S,
N_w – the number of eutectic cells that intersect the sides of S but not their corners,
F – the surface area of S.

The graphite eutectic cells have a granular microstructure, and it can be assumed that the spatial grain configurations follow the so-called Poisson–Voronoi model [9]. Then, a stereological formula can be employed for calculations of the spatial cell count N_g (spatial cell density), which yields the average number of eutectic cells per unit volume

$$N_g \cong 0.568\,(N_F)^{3/2} \tag{8}$$

Table 1 gives the chemical composition of the experimental cast irons. In addition, the experimental data on times after inoculation, cell count N_F and N_g, plates casting modules M, the minimum temperatures T_m for the eutectic transformation of cast iron, as well as maximum undercooling ΔT_m at the beginning of solidification are given in Table 2.

Table 1. Time after inoculation and chemistry for test series I

No. of castings	Time after inoculation, min	Chemical composition, wt. %				
		C	Si	Mn	P	S
I/1	base cast iron	3.25	1.17	0.13	0.085	0.047
I/2	1.5	3.14	1.98	0.13	0.091	0.067
I/3	5	3.18	2.05	0.11	0.093	0.061
I/4	10	3.16	2.04	0.13	0.095	0.065
I/5	15	3.21	2.01	0.14	0.095	0.053
I/6	20	3.20	2.08	0.13	0.098	0.050
I/7	25	3.16	2.08	0.13	0.091	0.052
Average composition		3.18	1.91	0.13	0.092	0.064

Table 2. Experimental results tests series I

No. of casting	Cell count		Module M	Eutectic temperature at the beginning of solidification T_m	Maximum undercooling	
Time after inoculation t_a – absolute t_d – relative T_i**	N_F	N			$\Delta T_m = T_s - T_m$	$\Delta T_{m,c} = T_s - T_{m,c}$*
	cm^{-2}	cm^{-3}	cm	°C	°C	°C
I/1 Base iron T_i = 1233°C	1075	20020	0.3	1123.7	35.1	32.4
	648	9369	0.5	1133.3	25.5	24.4
	324	3312	0.8	1138.0	20.8	19.1
	229	1891	1.1	1139.7	19.7	16.4
	99	559	1.5	1142.5	16.3	13.9

* See Eqs. (15), part I and Eqs. (15)–(18) part II.
** The mean temperature of the metal in the mold cavity just after pouring.

Table 2. cont.

No. of casting	Cell count		Module M	Eutectic temperature at the beginning of solidification T_m	Maximum undercooling	
Time after inoculation t_a – absolute t_d – relative T_i **	N_F	N			$\Delta T_m = T_s - T_m$	$\Delta T_{m,c} = T_s - T_{m,c}$ *
	cm^{-2}	cm^{-3}	cm	°C	°C	°C
I/2	2480	70150	0.5	1139.6	23.4	22.2
t_a = 1.5 min	893	15157	0.8	1146.9	17.2	18.1
t_d = 0.06	337	4092	1.1	1148.7	14.2	15.8
T_i = 1230°C	226	1930	1.5	1150.2	12.7	13.9
	2319	63472	0.3	1137.9	25.5	30.1
I/3	1773	42404	0.5	1139.7	23.7	23.6
t_a = 5 min	654	9500	0.8	1147.5	15.8	19.1
t_d = 0.20	256	2326	1.1	1147.0	16.3	16.8
T_i = 1248°C	185	1535	1.5	1150.2	13.1	14.9
	2277	61715	0.3	1131.7	31.5	31.8
I/4	1043	19133	0.5	1137.9	25.4	25.1
t_a = 10 min	612	8600	0.8	1146.5	16.8	20.5
t_d = 0.40	264	2436	1.1	1147.9	15.4	18.1
T_i = 1246°C	170	1259	1.5	1151.9	11.4	16.1
	2036	52181	0.3	1133.5	29.8	34.5
I/5	880	14828	0.5	1135.7	27.6	27.2
t_a = 15 min	364	3945	0.8	1143.0	20.3	22.3
t_d = 0.60	132	861	1.1	1144.0	19.3	19.6
T_i = 1230°C	59	257	1.5	1148.4	14.5	17.5
	1270	25707	0.3	1123.8	39.6	35.8
I/6	638	9153	0.5	1135.3	28.0	28.2
t_a = 20 min	176	2450	0.8	1137.8	25.7	23.2
t_d = 0.80	94	518	1.1	1144.5	18.8	20.4
T_i = 1252°C	52	213	1.5	1145.9	17.5	18.2

* See Eqs. (15), part I and Eqs. (15)–(18) part II.
** The mean temperature of the metal in the mold cavity just after pouring.

Table 2. cont.

No. of casting	Cell count		Module M	Eutectic temperature at the beginning of solidification T_m	Maximum undercooling	
Time after inoculation t_a – absolute t_d – relative T_i^{**}	N_F	N			$\Delta T_m = T_s - T_m$	$\Delta T_{m,c} = T_s - T_{m,c}^{*}$
	cm^{-2}	cm^{-3}	cm	°C	°C	°C
I/7 $t_a = t_r = 25$ min $t_d = 1.0$ $T_i = 1234$°C	950	16632	0.3	1122.1	41.4	42.7
	437	5012	0.5	1132.1	31.4	33.3
	175	1326	0.8	1137.6	25.8	26.9
	84	437	1.1	1142.0	21.5	25.6
	47	183	1.5	1145.0	18.5	20.9

* See Eqs. (15), part I and Eqs. (15)–(18) part II.
** The mean temperature of the metal in the mold cavity just after pouring.

The maximum degree of cast iron undercooling, ΔT_m for the individual plates, as well as temperature range ΔT_{sc} were determined from:

$$\Delta T_m = T_s - T_m \tag{9}$$

$$\Delta T_{sc} = T_s - T_c \tag{10}$$

where:

$$T_s = 1154 + 5.25\ \mathrm{Si} - 14.88\ \mathrm{P} \tag{11}$$

$$T_c = 1130.56 + 4.06\ \left(\mathrm{C} - 3.33\ \mathrm{Si} - 12.58\ \mathrm{P}\right) \tag{12}$$

In Eq. (9), T_m is the minimum temperature at the onset of solidification (as determined from the cooling curves, Fig. 3 [12]).

Small wedges (dimensions: B_w = 1.25 cm, $\beta = 28.5^{\circ}$, see Fig. 7 [12]) and samples for chemical composition were also cast simultaneously with the plates. Hence, after cutting the wedges, metallographic examinations were made by etching with the Stead reagent to reveal the eutectic cells boundaries. Figure 3 shows typical planar microstructures (on the specimen cross-section) of the wedges with distinct graphite eutectic cells.

The chilled iron at the apex of the wedge consisted of two zones:

1) the portion closest to the apex was entirely free of any gray spots and it was designated as a clear chill,
2) the portion starting at the end of the clear chill and continuing all the way down to the location were the last spot of cementite that is white iron is visible was designated as the mottled zone.

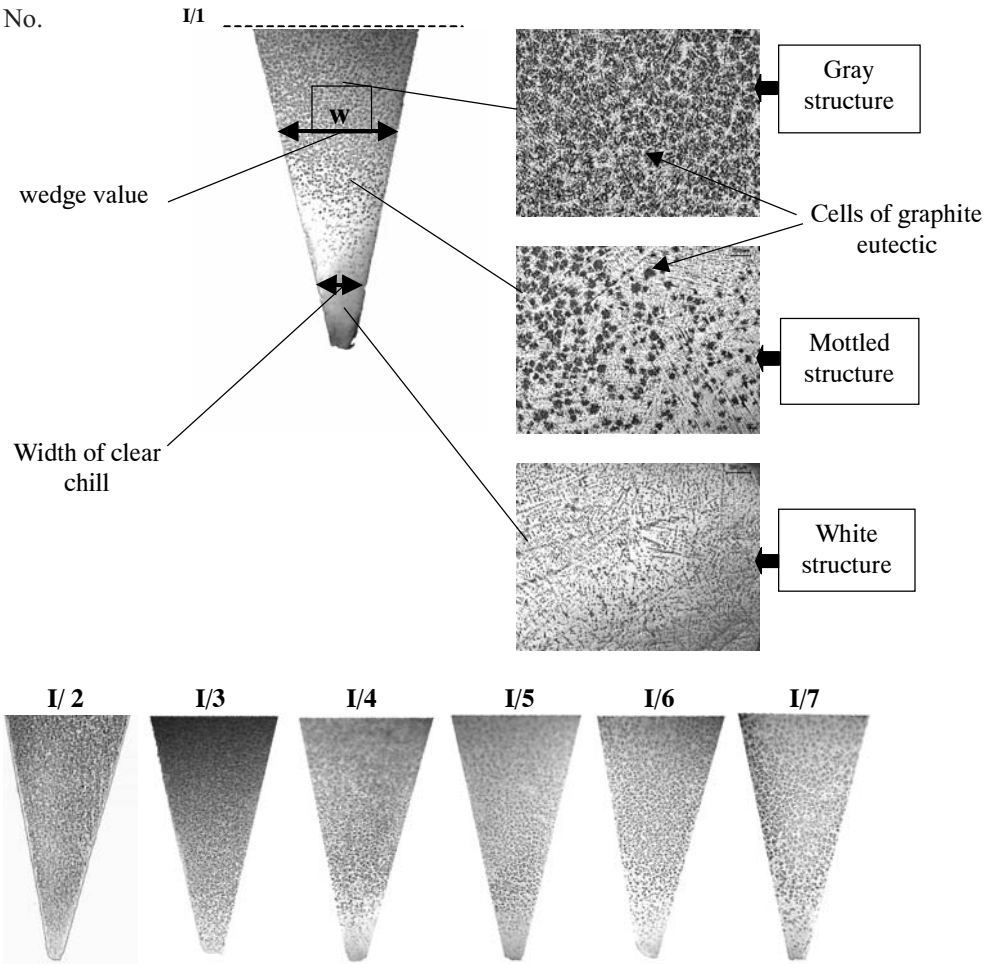

Fig. 3. *Exhibited microstructures in wedge shaped castings from test melts I/1–I/7*

The width, w of the total chill and the cell count N_F were measured at the junction of the gray cast iron microstructure with (the so called wedge value) the first appearance of chilled iron. The planar cell count N_F in the vicinity of that junction was converted into the volumetric cell count N using Eq. (8). The results of these measurements are given in Table 3.

Taking into account the chemical composition of the cast iron from the series I of tests (Tab. 1), the cell count (Tab. 3), the mean initial temperature T_i (Tab. 4), any relevant thermo physical data (Tab. 1 [12]) and using a wedge size coefficient n, which for small wedges is 0.87, the theoretical wedge value can be estimated from Eqs. (3) and (6). The results from these calculations are given in Table 4. Notice that comparisons between the theoretical and experimental results yield a rather good agreement.

Table 3. Experimental results tests series I (small wedge, B_w = 1.25 cm, b = 28.5°)

No. of casting	Time after inoculation t_a – absolute t_d – relative	Eutectic cell count N_F	Eutectic cell count N_g	Total wedge value w
		cm^{-2}	cm^{-3}	mm
I/1	–	2219	59372	7.9
I/2	t_a = 1.5 min t_d = 0.06	20566	1675225	3.3
I/3	t_a = 5 min t_d = 0.20	15828	1131065	3.6
I/4	t_a = 10 min t_d = 0.40	5113	207664	4.0
I/5	t_a = 15 min t_d = 0.60	4959	198353	4.5
I/6	t_a = 20 min t_d = 0.80	3893	137924	4.8
I/7	t_a = 25 min t_d = 1.0	2188	58133	5.5

Table 4. Experimental and estimated wedge values (small wedge, B_w = 1.25 cm, b = 28.5°)

No. of casting	Relative time after inoculation t_d	Measured wedge value, w	Calculated wedge value w		Calculated chilling tendency CT $s^{1/2}/°C^{1/3}$	
			Eqs. (3) and (6)	Eqs. (3), (5) and (15)÷(18)	Eq. (6)	Eq. (5)
	–	mm	mm		–	–
I/1	–	7.9	7.1	8.6	0.91	1.10
I/2	0.06	3.3	3.1	3.5	0.38	0.43
I/3	0.20	3.6	3.3	3.7	0.40	0.44
I/4	0.40	4.0	4.4	3.9	0.53	0.48
I/5	0.60	4.5	4.6	4.4	0.54	0.53
I/6	0.80	4.8	4.7	4.8	0.57	0.58
I/7	1.0	5.5	5.4	6.5	0.66	0.79
Mean temperature (just after pouring) of metal in mould cavity T_i = 1270 °C						

In addition, from Table 2 the inoculation effect can be inferred by the cell count as a function of the time t_a from the instant in which the inoculant was introduced into the melt. Notice that after 25 minutes (Fig. 4), the observed changes in the cell count are rather negligible and this time t_r can be considered as a reference point. Hence, the changes in the density of eutectic cells can be expressed as a function of a dimensionless time as

$$t_d = \frac{t_a}{t_r} \tag{13}$$

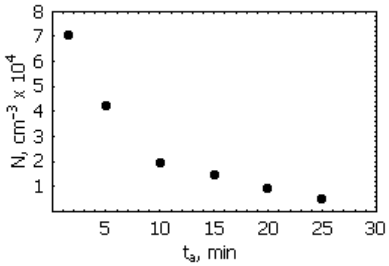

Fig. 4. *Effect of the time t after inoculation on the eutectic cells count N for a casting modules M = 0.5 cm, (s = 1.0 cm)*

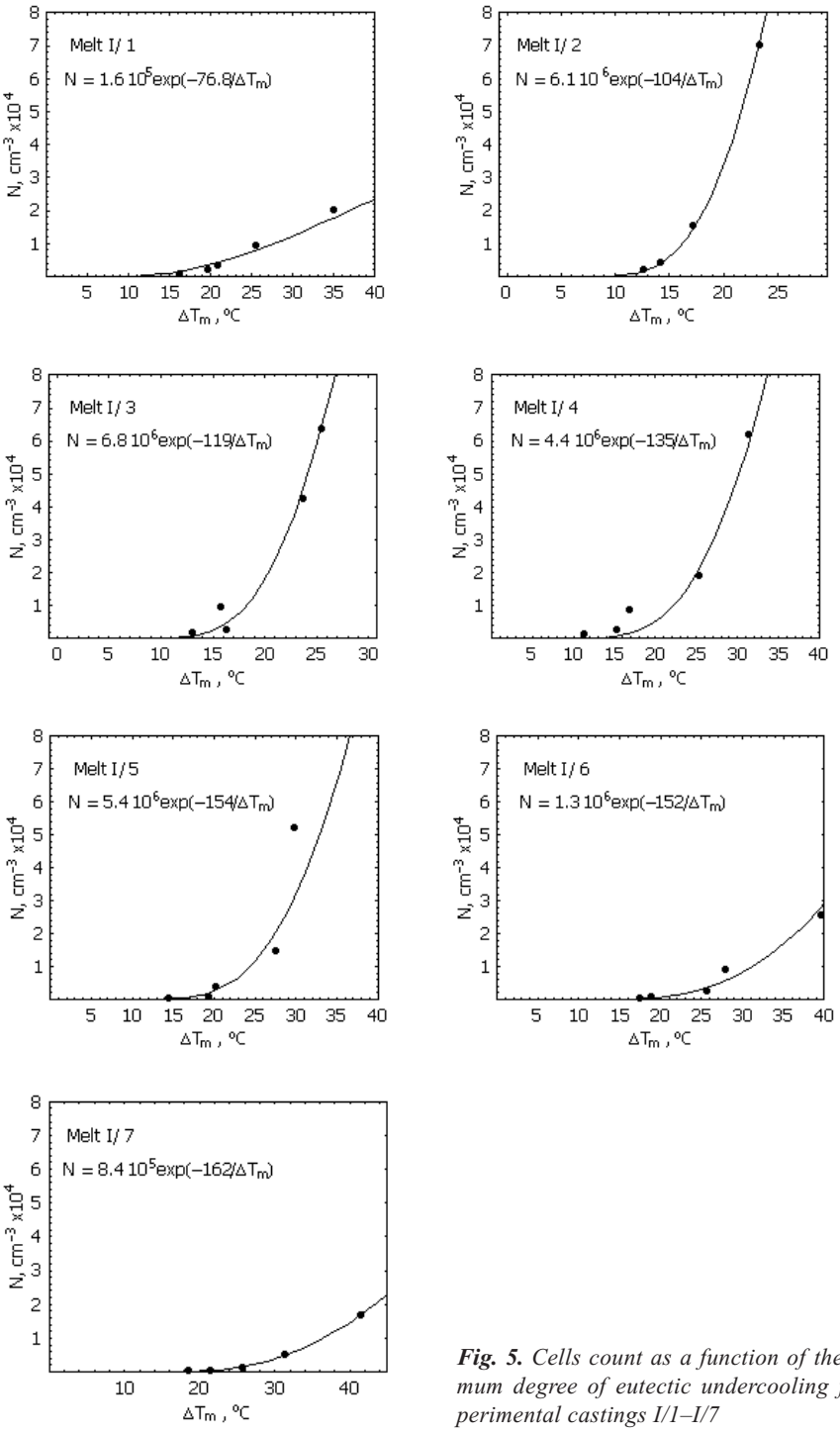

Fig. 5. *Cells count as a function of the maximum degree of eutectic undercooling for experimental castings I/1–I/7*

In addition, from Table 2 it is clear that the cell count not only depends on the time t_i but also on the maximum undercooling ΔT_m. Figure 5 shows the experimental results for cell count N plotted against ΔT_m for various dimensionless times t_d. Notice from these figures that N is exponentially increasing function of the maximum undercooling

$$N = N_s \exp\left(-\frac{b}{\Delta T_m}\right), \text{ cm}^{-3} \tag{14}$$

From Figure 5 it is apparent that for inoculated cast iron, N_s and b in equation (14) are time dependent. The empirical dependence of N_s and b as a function of time t_d is shown in Figure 6.

A polynominal approximation indicates that the regression curves are of the form for:

– the inoculated cast iron:

$$b = 96.9 + 122.6\, t_d - 59.2\, t_d{}^2, \text{ °C} \tag{15}$$

$$N_s = 10^6 \left(6.5 - 0.8\, t_d - 5.3\, t_d{}^2\right), \text{ cm}^{-3} \tag{16}$$

– the base cast iron prior to inoculation:

$$b = 76.8, \text{ °C} \tag{17}$$

$$N_s = 1.6 \cdot 10^5, \text{cm}^{-3} \tag{18}$$

Taking into account the chemical composition of the cast iron (Tab. 1), the expressions for N_s and b, Eqs. (15)–(18), the casting modules of the plates M, the mean temperature of the metal in the mould cavity just after pouring, T_i (Tab. 2) and any relevant thermophysical data (Tab. 1 [12]), the maximum undercooling ($\Delta T_m = T_s - T_m$) was calculated (Eq. (15) [12]). A comparison (see Tab. 2) between the experimentally measured and the calculated degrees of undercooling shows that there are no significant differences. In addition, if one takes into account Eqs. (3) and (6), and N from Table 3, chilling tendency CT and the total wedge value w in the wedges can be found as a function of the dimensionless time t_d. Similar results can be obtained by means of Eqs. (3), (5), and (15)–(18). The results from these calculations are given in Table 4 and Figure 7.

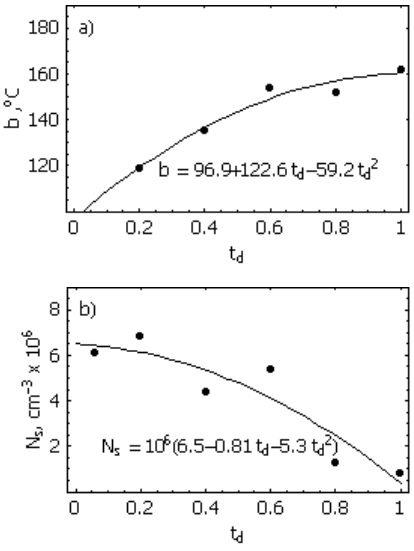

Fig. 6. *Effect of the dimensionless time t_d after inoculation on coefficients: b (a) and N_s (b)*

The results from the calculations made using Eq. (47), part I and from the data in Table 1 [12] and Table 2 are shown in Figure 8. In particular, the solid line in this figure corresponds to cast iron of average chemical composition (Tab. 1), and hence with average values for T_s.

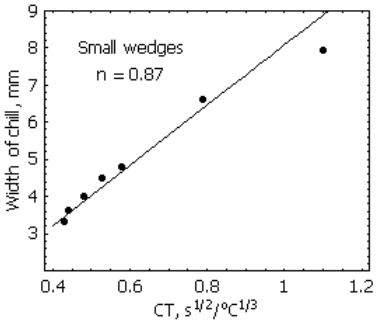

Fig. 7. *Effect of chilling tendency CT on the wedge value*

It is well known that under constant wall thickness conditions (s = const.), ΔT_m and N depend on the physicochemical state of the liquid cast iron, which in turn is influenced by the various inoculation treatments, time after inoculation and chemical composition. From Table 2 (see also points, Fig. 8) it is found that under constant wall thickness, as the maximum degree of undercooling increases, the cell count decreases. Therefore, it can be concluded that the experimental data are in good agreement with the predictions of Eq. (47) [12].

Combining Eqs. (50) and (53) [12], spatial cell count can also be determined from

$$N_g = \frac{N_s}{\exp\left[8\,\mathrm{ProductLog}\left(y\right)\right]} \tag{19}$$

where y – see Eq. (54) [12].

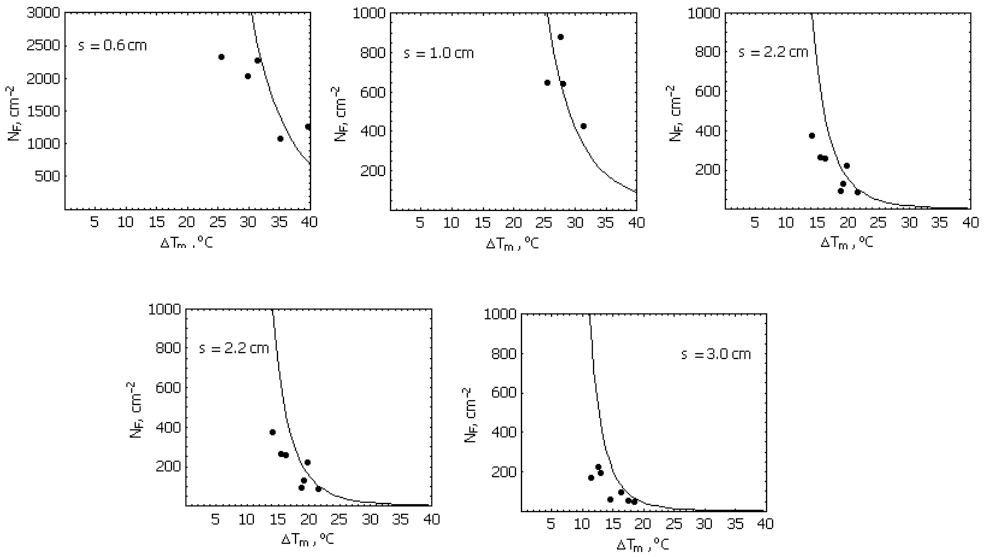

Fig. 8. *Cell count as a function of maximum undercooling: experimental results, results based on Eq. (47) [12]*

Moreover, considering the nucleation parameters b and N_s given by Eqs. (15) and (16), and taking into account average chemical composition of cast iron (Tab. 1), as well as data from Table 1 [12] and the mean temperature of the metal in the mold cavity just after pouring, T_i (Tab. 2), together with Eq. (19), calculations were made of the effect of wall thickness on the cell count. Accordingly, the results from these calculations are shown in Figure 9 with solid lines. Also, for comparison purposes the experimental results are included in this figure. Once again, there is good agreement between the experimental outcome and the predictions of the proposed theoretical analysis.

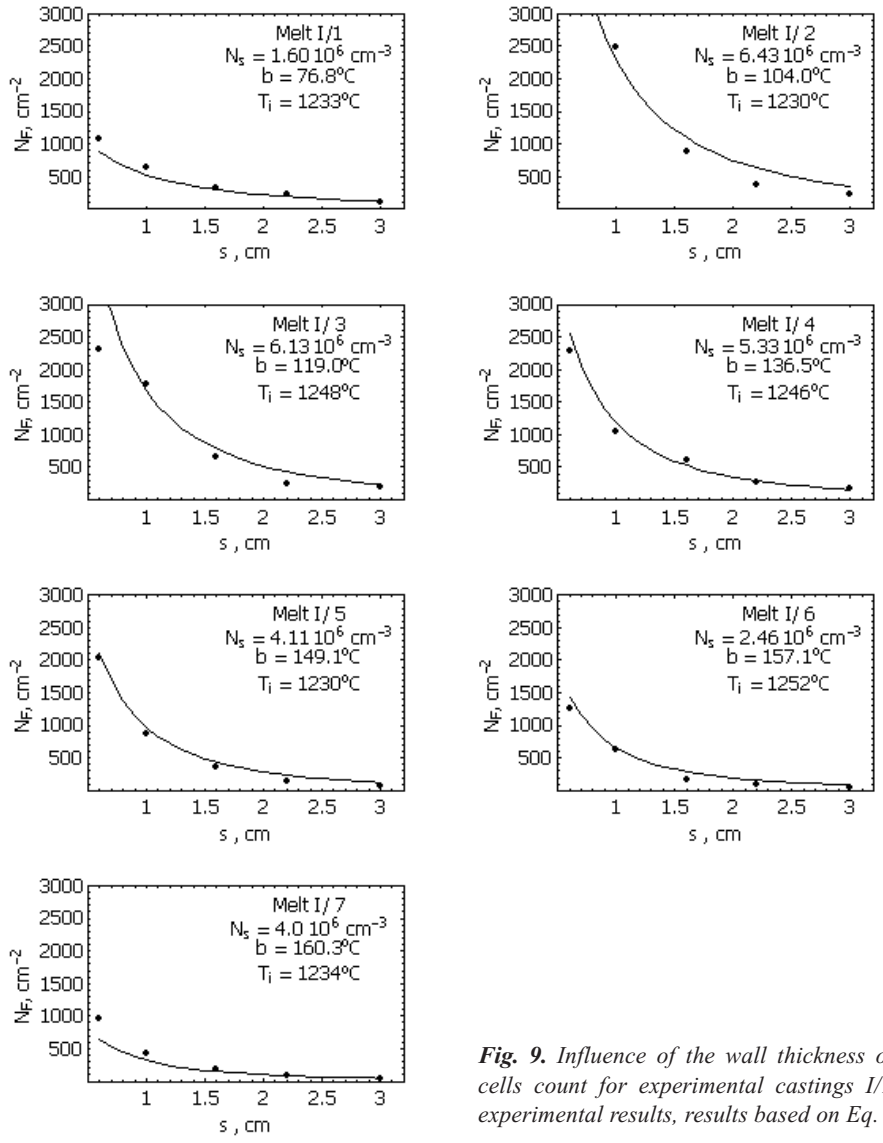

Fig. 9. *Influence of the wall thickness on the cells count for experimental castings I/1–I/7: experimental results, results based on Eq. (19)*

Big wedges – Series II

The experimental melts were made in the electric induction furnace mentioned before (test series I). The charge materials for the furnace consisted of pig iron, steel scrap, commercially pure silicon, and ferro-phosphorus. After melting of the charge and superheating to 1400°C, large wedges of the Meehanite type (dimensions: B_w = 2.5 cm and $\beta = 25^o$) were cast. From each melt, a sample was taken for chemical composition. A Pt-PtRh10 thermocouple was inserted in the center of the wedge cavity in the mold (from quartz sand) to record the initial temperature T_i. The results of chemical composition, density of eutectic cells in wedges near the transition from gray to mottled cast iron (near T_c temperature), the wedge value and the mean temperature T_i are given in Table 5.

Table 5. Real and estimated data, tests series II (large wedge B_w = 2.5 cm, $b = 25^o$)

No. of melt	Chemical composition			Eutectic cell count N	Measured wedge value w	Calculated* wedge value w	Calculated* chilling tendency CT $s^{1/2}/^oC^{1/3}$
	C	Si	P				
	%			cm^{-3}	mm	mm	–
II/1	3.52	2,06	0.07	3070	7.8	8.3	1.1
II/2	3.43	1.92	0.07	7247	7.0	6.9	0.99
II/3	3.32	1,83	0.07	3671	8.6	7.4	1.14
II/4	3.56	1.75	0.07	2436	7.6	9.2	1.26
II/5	3.50	1.74	0.07	1107	10.7	10.1	1.44
II/6	3.45	1.66	0.07	1338	10.0	9.7	1.43
Mean temperature (just after pouring) of metal in mould cavity T_i = 1278 °C. * Equations (3) and (6) were used for calculations.							

In the case of large size wedges, the wedge size coefficient n is 0.68. From the chemical composition, cell count, initial temperature T_i, as well as thermophysical data (Tab. 1 [12]), chilling tendency of cast iron CT and the wedge value w for the wedges was calcula-ted using Eqs. (3) and (6). The results of these calculations are given in Table 5 and Figure 10. Notice that again there is rather good agreement between the theoretical calculations and the experimental outcome.

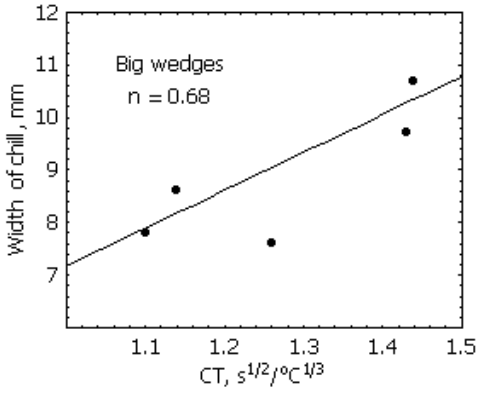

Fig. 10. *Effect of chilling tendency on the wedge value*

3. THIN-WALL SAND CASTINGS

A recent trend in the design of vehicle components has been focused in the production of thin-walled sand castings in order to save materials and energy. These castings due to the relatively small volume to surface ratios (small casting modulus) solidify at high rates leading to the development of chills. Most production efforts on thin-walled casting have been focused on metal chemistry, inoculation, and gating system. However, decrease of the material mould ability to absorb of heat may have the potential to significantly reduce the casting wall thickness far better than by any other efforts. This can be easily confirmed by making some estimations based on Eqs. (2), (4), (5), (10) (15), (16) and (21), (28), (64) [12] for base cast iron and cast iron directly after the inoculation treatment (t_d = 0.06). Figure 11 shows the critical wall thickness s_{cr} (see Eq. (64) [12]) of a casting when the chill is formed. From this figure, it can be observed that the effect of the mold material ability to absorb heat a on the critical wall thickness s_{cr} of the casting when the chill is formed is very significant (see also Tab. 6).

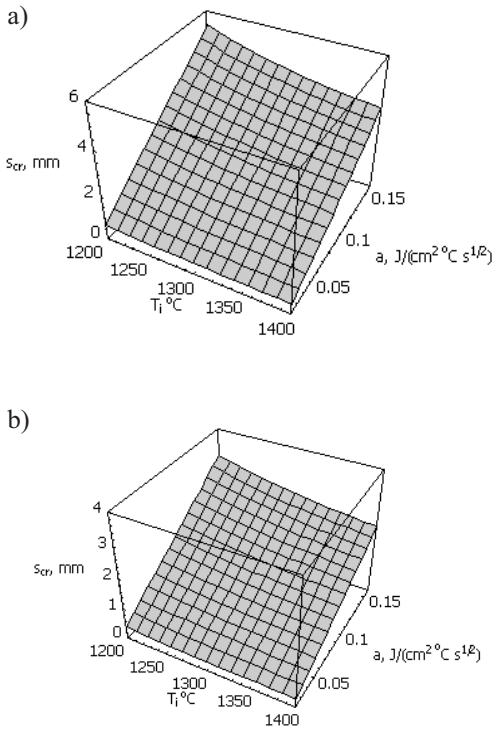

Fig. 11. *Critical wall thickness s_{cr} of a casting when a chill is formed: a) base cast iron; b) inoculated cast iron*

Table 6. Heat absorption data for moulds [10, 11] and critical plate wall thickness s_{cr}

Mould material	Ability of moulding material to absorb heat a	Critical wall thickness s_{cr}	
		Base cast iron	Inoculated cast iron
	J/(cm^2·°C·s$^{1/2}$)	mm	
Quartz sand	0.08 ÷0.12	2.7÷4.7	1.1÷1.7
Olivine	0.1	3.5	1.4
Chromite	0.15	5.2	2.2
Zircon	0.13÷0.15	4.5÷5.2	1.8÷2.2
LDASC, Ashland	0.018÷0.03	0.6÷1	0.2÷0.4
Initial temperature of metal in mould cavity T_i = 1400°C			

4. CONCLUSIONS

The theory for the chill of cast iron was described in [12] of this work, and in this work, the chilling tendency was verified experimentally. In particular, it has been shown that the results of calculations on the chill formation using data from direct measurements of eutectic cell count in wedge shaped casting (Tab. 3) using Eqs. (3) and (6), as well as measurements of eutectic cell count in plates (Tab. 2) from the same melt and through the use of equations (3) and (5) as well as (15)–(19) yield results that are in good agreement with experimentally measured values. It has been also concluded through appropriate calculations that besides any metallurgical factors, the chill is significantly affected by the moulding material ability to absorb heat a. Reducing a to the value of roughly 0.04 J/(cm^2 ·s$^{1/2}$·^{o}C) will enable the production of castings with wall thicknesses about of 0.1 cm without the development of a chill.

This work was supported by Statutory Grant No. 11.11.170.250 and made in Department of Cast Iron AGH, Cracow, Poland.

REFERENCES

[1] *Kubick E.J., Javaid A., Bradley F.J.*: Investigation of Effect C, Si, Mn, S and P on Solidification Characteristics and Chill Tendency of Gray Iron – Part II: Chill Tendency. AFS Transaction, 103 (1997), 579–586

[2] *Fraś E., Serano T., Bustos A.*: Fundiciones de hierro. ILAFA, Chile, 1990

[3] *Elliott E.*: Cast Iron Technology. Butterworths, London, 1988

[4] *Merchant H.D.*: Solidification of Cast Iron. In: Recent Research on Cast Iron, Gordon and Breach, Merchant H. (Eds), Science Publishers, New York, 1968, 1–100

[5] *Kubick E.J.*, *Javaid A., Bradley F.J.*: Investigation of effect of C, Si, Mn, S and P solidification characteristic and chill tendency of gray iron – Part I: Thermal Analysis Results. AFS, Transactions, 105 (1997) 573–578

[6] *Fraś E., Wiencek K., Górny M., Lopez H.*: Nucleation and grain density – a theoretical model and experimental verification. Archives of Metallurgy, 46 (2001), 317

[7] *Fraś E., Górny M., Tartera J.*: Nucleation and grain density – a theoretical model and experimental verification. International Journal of Cast Research, 16 (2003), 99

[8] *Ryś J.*: Stereology of materials. Fotobit, Cracow, 1995

[9] *Osher J., Lorz.*: Quantitative Gefuengenanalysie. DVG Leipzig-Stuttgard, 1994

[10] *Showman R.E., Aufderheide R.C.*: A process for thin-wall sand castings. AFS Transactions, 111 (2003), 567–578

[11] *Fredriksson H., Svensson H.*: Computer simulation of the structure formed during solidification of cast iron. The Physical Metallurgy of Cast Iron, Fredricsson H., Hillert M. (Eds), North-Holland, New York, 1985, 73–284

[12] *Fraś E., Górny M., López H.F.*: Solidification conditions of gray and white cast iron. Part I – theoretical background. Metallurgy and Foundry Engineering, 31 (2005) 1, 13–35

Received
January 2005